Tunable Source for THz Spectroscopy

Abstract: We have developed a terahertz spectrometer based on difference frequency generation of beams from an ytterbium fiber Master Oscillator Power Amplifier system. The spectrometer has a resolution of ~2 GHz. It can be tuned rapidly over several hundred GHz, and a wider frequency range can be covered (0.7-2.5 THz demonstrated) by swapping in alternate seed lasers and adjusting the alignment of the beams into the DFG crystal. The system was constructed entirely from commercially available fibre and fibre components. We present some demonstration data on water vapor absorption lines.

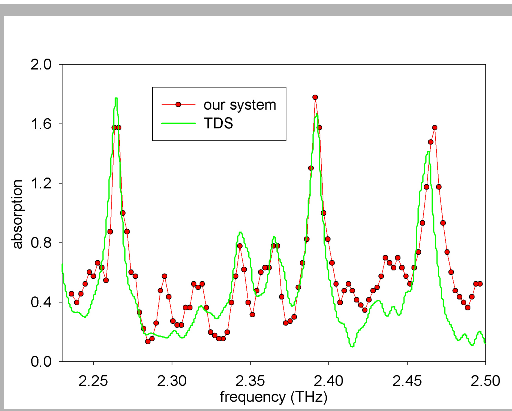

Spectral data (water vapour absorptions) collected via fiber MOPA seeded DFG (red) compared with data from Time Domain Spectroscopy (green).

Fiber MOPA Based Tunable Source for Terahertz Spectroscopy

A. Malinowski[1], *D. Lin*[1,*], *S.U. Alam*[1], *Z. Zhang*[1], *M. Ibsen*[1], *J. Young*[2], *P. Wright*[2], *K. Ozanyan*[2], *M. Stringer*[3], *R.E. Miles*[3] *and D.J. Richardson*[1,*]

[1] Optoelectronics Research Centre, University of Southampton, Southampton, SO17 1BJ, United Kingdom

[2] School of Electrical and Electronic Engineering, University of Manchester, Manchester M13 9PL, United Kingdom

[3] Institute for Microwaves and Photonics, University of Leeds, Leeds LS2 9JT, United Kingdom

Received X Month, XXXX; revised X Month, XXXX; accepted X Month, XXXX;
Published online: X Month, XXXX

Key words: fiber laser; THz generation

PACS: 42.55.Wd, 42.65.Ky

1. Introduction

Pulsed fiber MOPAs have received increasing attention over the past decade offering potential advantages in terms of efficiency, compactness, reliability, ease of thermal management and high average power levels relative to existing pulsed laser approaches [1]. Such sources are ideal for a diverse range of frequency conversion applications offering novel system opportunities spanning the soft X-ray to THz frequency regimes.

The THz spectral range is becoming of increasing interest for a range of emerging applications in sensing, imaging and basic science. However, reliably generating and detecting radiation in this spectral regime has been challenging. Narrow-linewidth high-intensity THz radiation, tuneable over a wide frequency range, has been produced by Difference Frequency Generation (DFG) from ~1.06 µm laser sources using a variety of nonlinear crystals [2]. The resulting THz beam is diffraction-limited and highly coherent. The THz linewidth and frequency stability are determined by those of the laser sources with linewidths as narrow as a few MHz achieved. Pulsed single-frequency DFG THz sources usually employ a Q-switched master laser, typically Nd-YAG, and a

* Corresponding author: e-mail: djr@orc.soton.ac.uk

frequency-shifted tunable optical parametric oscillator (OPO). However, these represent relatively bulky and complex systems. THz generation via DFG with a fiber laser system has recently been demonstrated [3, 4] and used for imaging applications [5] promising significant benefits in terms of source size and performance, as discussed previously.

For a THz system to be useful for spectroscopy, it requires both frequency tunability and a narrow linewidth. Here we demonstrate a THz spectrometer based on difference frequency generation (DFG) of the outputs from a dual fiber MOPA system, which provides GHz resolution and a broad tuning range. The source also provides the ability to switch rapidly between multiple frequencies to facilitate real time THz tomography applications. We demonstrate its performance by measuring the absorption features of water vapor in air.

2. System setup

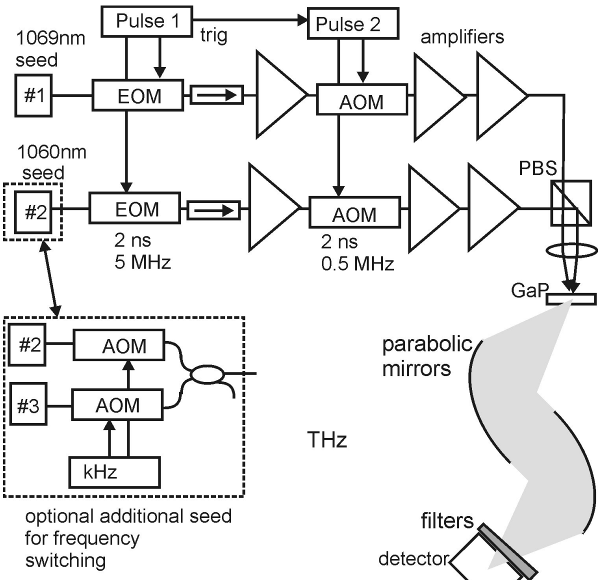

Figure 1 Schematic of dual fiber MOPA system and THz generation.

Fig. 1 shows the configuration of the pulsed MOPAs and non-collinear THz generation in GaP crystal. Two independent MOPA chains are used to generate the two required wavelengths. The two amplifier chains were essentially identical. The system was fully fiberised with the exception of the pump launch to the final amplifier stage, which was end pumped.

It is possible to generate both inputs in the same amplifier chain. This is a simpler approach, but has a number of disadvantages. Propagating both wavelengths in the same amplifier chain significantly exacerbates problems due to nonlinear optical effects. Cross phase modulation (XPM) will add to the spectral broadening and Four-Wave Mixing (4WM) results in the diversion of optical power to undesired wavelengths. In addition, for the frequency range we are considering (~2.5 THz), THz generation is calculated to be about 8 times less efficient for co-linear generation than for correctly phase-matched non-collinear generation, so it is desirable to have independent outputs.

The seeds were distributed feedback fiber lasers (DFBs) with kHz linewidths and output powers of ~20mW, fabricated in the ORC. The DFBs were attached at one end to piezo-controlled translation stages for strain tuning, by which we tuned them from their unstrained wavelengths by up to about 0.7nm. The seed lasers used to demonstrate the spectroscopic performance of the system had unstrained wavelengths λ_1= 1069 nm , λ_2=1060 nm, yielding an unstrained difference frequency of 2.4 THz, and a tuning range of about +/- 0.2 THz. The MOPA output wavelengths were monitored by a high resolution OSA during measurements.

The outputs of the seed lasers are connected to the next component of the system by means of standard FC/APC screw connectors, so that seeds with other wavelength ranges can be swapped in rapidly. By replacing seed #2 with the arrangement shown in the inset of figure 1, we can switch rapidly between pairs of frequencies by modulating the transmission of the AOMs, allowing real time comparison of signals at different frequencies.

The outputs from the seeds were modulated by Electro-Optic Modulators (EOMs) such that a train of pulses were formed and then launched into the amplifier chain. The EOM had an extinction ratio of better than 45 dB. In the experiments described here the pulses had 2ns duration and the repetition rate was 5 MHz (corresponding to a duty cycle of 1/100). The average output power after the EOM was typically around 50-100μW. The seeds were fabricated with non-PM fiber. Fiberised polarization controllers were used to align the polarization state of the output from the seeds with the slow axis of the input fibre of the EOMs, which are single polarization devices. From the EOMs onwards, all fibre and components in the system are polarization maintaining.

The single-polarization outputs from the EOMs were then amplified by a 1st stage pre-amplifier, which comprised a 2.5m long core-pumped, Yb-doped SM PM Nufern fibre with a core diameter and NA of 6μm and 0.12 respectively. The amplifier was bi-directionally pumped with 975nm SM laser diodes. The typical output from the 1st stage pre-amplifier was 10-20mW in power.

This output of the 1^{st} amplifier stage was gated by an AOM. The gating time of the AOM was about 20ns. The AOM was used as a pulse picker to give a repetition rate of 500 kHz (duty cycle: 1/1000). It also suppressed ASE output from the first stage preamplifier.

The 2nd stage preamplifier was a cladding pumped SM PM Yb-doped Nufern fiber with a core/cladding diameter and NA of 6μm/125μm and 0.12/0.45 respectively. The fiber was co-pumped by a 915nm fiber-pigtailed broad-stripe diode laser through a fused

Tapered Fibre Bundle (TFB). The length of the active medium was chosen to be ~5m so that requirements of nonlinearity management and short-wavelength ASE suppression were balanced. Fast axis blocking PM isolators, as well as protecting the amplifier components, help to maintain a high Polarization Extinction Ratio (PER) through the amplifier chain.

The final stage amplifier was a 5.5m long PM Yb-doped Nufern fiber with a core/cladding diameter and NA of 25µm/350µm and 0.055/0.45 respectively. SM operation was implemented by tapering the input cladding end of the fiber to a diameter of 125µm, which was spliced directly with the output of the 2nd stage preamplifier. Tapering also reduced the splice loss from the 2nd stage output to the final stage input. The amplifier was end-pumped using a number of commercially available reflection-protected 975nm diodes (combined by a TFB). This mode of pumping was chosen because it offers a shorter effective amplifier length than forward pumping with an inline TFB, and therefore limited nonlinear spectral broadening effects in the amplifier. To prevent the damage to the end facet, a 1.5mm long 350µm diameter dummy fiber (end-cap) was spliced to the output of the gain fiber and it was angle (7^o) polished to avoid backward reflection. A dichroic mirror was used to separate the signal and pump beams.

The MOPA outputs with the wavelengths of λ_1 and λ_2 were mixed with orthogonal polarization using a polarizing beam splitter (PBS) and focused by a lens (spot size: ~200µm) onto a DFG crystal. We used a 2mm thick GaP crystal cut in (110) orientation. Thicker GaP crystals are available commercially, as are nonlinear crystals with higher effective nonlinearity (e.g. GaSe). The crystal type and thickness was chosen to allow DFG over a relatively broad bandwidth without realignment of the crystal. The minimum useable spot size is determined by the divergence of the THz beam and the NA of the THz collecting optics (0.5 rad). Assuming a Gaussian beam, at 2.4 THz we expect a divergence of about 0.4rad for a 200 µm spot. A half wave plate (HWP) was used to adjust the polarization of the MOPA output so as to obtain the maximum THz power.

GaP is not birefringent; phase matching is achieved by using the correct wavelengths of input beams (around 975nm For DFG to 2.5 THz[6]), or by means of non-collinear alignment of the input beams [7]. At lower THz frequencies the phase matching conditions are less tight and our wavelengths are close enough to the optimum values for a reasonably efficient collinear generation. . However, for efficient generation around 2.5 THz we require the non-collinear alignment. Because of the much smaller wavenumber of the THz beam compared to the IR beams, the THz output angle is much larger than the angle between the two input beams. For a 2 mm GaP crystal utilising non-collinear phase matching, the phase matching bandwidth is ~1 THz for peak ~2.4 THz. We tuned the angle between the two beams by translating the PBS to obtain maximum signal. The external angle between the two input beams for optimal phase matching is of order 0.5^o, whilst the output angle is about 40^o.

The THz signal was collected using a pair of gold-coated parabolic mirrors. The first mirror (diameter 50mm, focal length 50mm) was used to collimate the beam. A second mirror (diameter 50mm, focal length 100mm) was used to focus the beam onto a Golay cell. A large proportion of the IR radiation was transmitted through the GaP crystal. Most of this was picked off with a small mirror onto a beam dump. To additionally reduce the effect of scattered laser light, a 12.5mm wedged silicon window was placed in front of the detector to block the unabsorbed laser light. This reduced the amount of THz reaching the detector by ~50% (due to reflections from the silicon surfaces), but reduced the scattered laser radiation reaching the detector by several orders of magnitude.

3. System performance

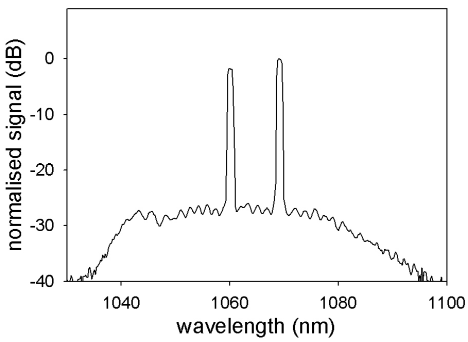

Figure 2 Spectrum of combined outputs of MOPAs (1 nm resolution).

Figure 2 shows the combined spectra from the two MOPAs, each with average output powers of 4.5 W (peak powers of 4.5 kW), measured after the PBS. Output power was limited by the available pump power. Each had a polarisation extinction ratio (PER) of ~15 dB and a measured M^2~1.1. The optical signal to noise ratio (OSNR) was >25 dB. Performance was not detectably different when the seed-switching shown in the inset of figure 1 was implemented. The first stage amplifiers were signal saturated so the additional losses introduced by the switching arrangement had no significant effect.

We were unable to resolve the spectral width with the OSA available to us (0.01nm resolution), so the spectral bandwidths are less than 3 GHz. The estimated true bandwidth based on the pulse duration and Self-Phase-Modulation (SPM) calculations was ~1 GHz.

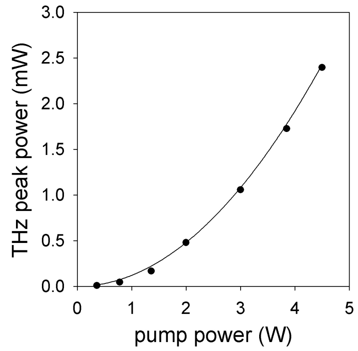

Figure 3 THz peak power vs. MOPA power (both MOPAs with equal power),

The other nonlinear effects which generally need to be considered in pulsed fiber MOPAs are Stimulated Raman Scattering (SRS) and Stimulated Brillouiun Scattering (SBS)[8]. The calculated SRS threshold for these amplifiers is several tens of kW, and was not observed. SBS can be significant for narrow-linewidth systems, but has a build-up time of several nanoseconds, so is not an issue with the 2 ns pulses we used for these experiments. SBS was only observed, in the form of intermittent backward travelling pulses, when pulse duration was increased above ~3 ns.

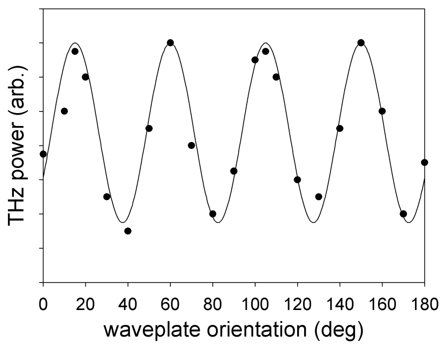

Fig 4 Experimental (points) and theoretical (line) polarisation orientation dependence of THz power.

All our THz measurements were taken in ambient air over a path length of ~240mm. Measurements of the performance of the THz generation system were taken at 2.5 THz where atmospheric absorption is fairly low. Fig. 3 shows a plot of THz power generated vs. the MOPA power (both MOPAs had the same output power in these experiments). At 4.5 kW average MOPA power the peak THz power generated (allowing for known losses in the filters on the detector) was found to be 2.4 mW (average power 2.4 µW). This is about an order of magnitude less than we expect using the plane wave approximation [3, 9] and known materials constants [10], and assuming optimum phase matching, but given the divergence of the THz beam and significant mutual angle between the THz and IR beams reducing the overlap, as well as possible losses in the collection of the THz radiation, this seems a reasonable value.

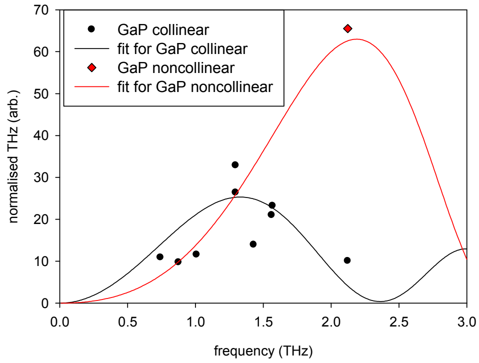

Figure 5 THz generation at various frequencies using various pairs of seed lasers. Black squares: collinear beam propagation, red diamond: optimised noncollinear beam angle. The curves show the theoretical predictions of the associated tuning curves for both beam configurations (assuming the same experimental pump powers and normalised to the average signal strength in both cases). The scatter in data points for the collinear case is likely due to atmospheric absorption in the beam path from crystal to detector, which could not be accounted for because the other lasers used were not as spectrally clean and stable as those used to collect the data at 2.4 THz.

THz power generated by DFG from orthogonal polarisation components in (110) GaP is expected to have a $\cos^2 2\theta + \frac{1}{4}\sin^2 2\theta$ dependence on polarisation orientation of the incident beams with respect to the crystal orientation [11]. Fig. 4 shows power generated as a function of the orientation of the waveplate which set the polarisation of the incident beams. The solid line shows the expected dependency of the THz power on orientation .

With other seed lasers we have demonstrated THz generation over the range 0.7-2.4 THz, as shown in Fig. 5. Not all seeds used in these measurements were tunable or narrow/single line, which means we were not able to consistently tune away from absorption lines, which may explain the broad distribution of the data points. Fig. 5 also shows the advantage of non-collinear generation for higher frequencies.

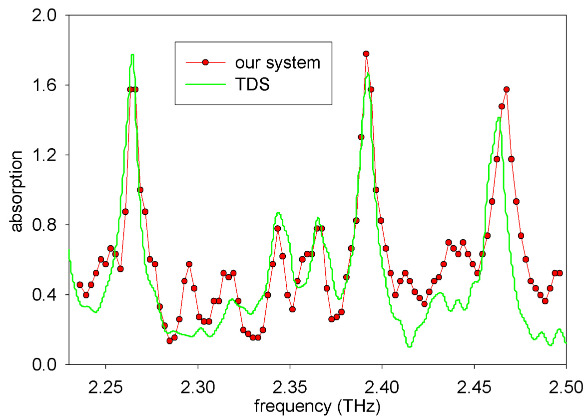

Figure 6 Spectral data (water vapour absorptions) collected via fiber MOPA seeded DFG and a pyroelectric detector (red with points), compared to data obtained via THz Time Domain Spectroscopy (green)

As a demonstration of spectrometer performance we measured the water absorption lines in ambient air. Tuning was achieved using the piezo-controllers. The THz frequency was determined by automated registration of the wavelengths of the lasers by a high resolution OSA. Figure 6 shows the absorption spectrum we obtained. Based on the bandwidths of the MOPAs, the spectral resolution should be better than 2 GHz. This is less than the width of any of the features in this spectrum (~10 GHz). We obtained an OSNR of 20 dB over a tuning range of ~0.4 THz (limited by the level of strain we were prepared to risk on the DFB fiber laser seeds). A trace obtained with a conventional Time Domain Spectroscopy (TDS) system under similar conditions [12] is shown for comparison, showing good agreement between the two techniques. The heights and widths of the main absorption peaks are well reproduced.

4. Conclusion

We have successfully demonstrated a THz spectrometer based on DFG seeded by a fiber MOPA system. The system was constructed from commercially available fiber. We have demonstrated spectroscopic performance utilizing water absorption in ambient air. We can tune smoothly across a range of approximately 0.3 THz using piezo-controllers. Spectral resolution is of order 2 GHz. We have demostrated THz generation in the range 0.7 – 2.5 THz. Peak THz power was 2.4 mW (average power of 2.4 μW). Rapid switching between two different THz frequencies for real-time tomography applications is possible simply by suitable gating of the three different seed diodes. Without realignment of the incident pumps, the spectrometer can rapidly access a frequency range of about a THz.

Acknowledgements This work was supported by EPSRC (Grant Number EP/E057292/1).

References

[1] D. J. Richardson, J. Nilsson, and W. A. Clarkson, J. Opt. Soc. Am. B **27**, B63 (2010).
[2] Y. J. Ding, W. Shi, J. Nonlinear Opt. Mat. and Phys., **4**, 557 (2003).
[3] D. Creeden, J.C McCarthy., P.A Ketteridge, *et. al.*, IEEE J. Sel. Top. Quant. Elect. **13,** 732-7 (2007)
[4] W. Shi, M. A. Leigh, J. Zong, Z. Yao, D. T. Nguyen, A. Chavez-Pirson, N. Peyghambarian IEEE J. Sel. Top. Quant., **15**, 377 (2009).
[5] D. Creeden, J. C. McCarthy, P. A. Ketteridge, P. G. Schunemann, T. Southward, J. J. Komiak, E. P. Chicklis, Opt. Express **15**, 6478 (2007).
[6] T. Taniuchi and H. Nakanishi, Electronics Letters, **40**, 60-62, (2004).
[7] T. Tanabe, K. Suto, J. Nishizawa T. Kimura and K. Saito, J. Applied Physics, **93**, 4610, (2003).
[8] G. P. Agrawal, *Nonlinear Fiber Optics*, 3rd. edn., Academic Press, New York, 2001.
[9] Y. R. Shen*, Nonlinear Infrared Generation*. New York: Springer, 1977.
[10] T. Taniuchi and H. Nakanishi, J. Applied Physics, **95**, 7588 (2004).
[11] Q. Chen, M. Tani, Z. Jiang, and X.-C. Zhang, J. Opt. Soc. Am. B, **18**, 823, 2001.
[12] P. U. Jepsen, D.G. Cooke and M. Koch, Laser and Photonics Reviews, **5**, 124-166, 2011.